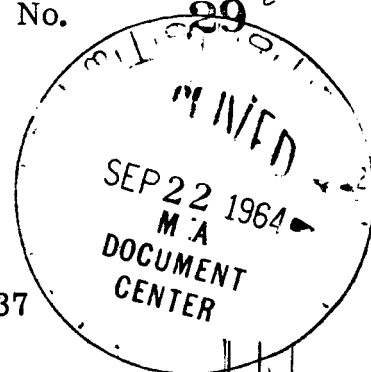


DO NOT REMOVE THIS COPY *Ref*

265.12384 Copy No. 89



NASA Program Apollo Working Paper No. 1137

STATIC AND DYNAMIC STABILITY CHARACTERISTICS OF THE
APOLLO LEV CANARD-POST ABORT CONFIGURATION (v)
N79-76484

(NASA-TM-X-66803) STATIC AND DYNAMIC
STABILITY CHARACTERISTICS OF THE APOLLO LEV
CANARD-POST ABORT CONFIGURATION (NASA) 39 p

Unclas

00/18 11568

FF No. 601	NASA-TM-X-66803	
	(NASA CR OR TMX OR AD NUMBER)	(CATEGORY)
[REDACTED]		
[REDACTED]		

CLASSIFIED DOCUMENT - TITLE UNCLASSIFIED

This material contains information affecting the national defense of the United States within the meaning of the espionage laws, Title 18, U. S. C., Secs. 793 and 794, the transmission or revelation of which in any manner to an unauthorized person is prohibited by law.

DISTRIBUTION AND REFERENCING

This paper is not suitable for general distribution or referencing.
It may be referenced only in other working correspondence and documents by participating organizations.



NATIONAL AERONAUTICS AND SPACE ADMINISTRATION
MANNED SPACECRAFT CENTER

Houston, Texas

September 14, 1964


CLASSIFICATION CHANGE

To UNCLASSIFIED

By authority of *Adm. 2-11-64* Date *11/1/64*
Changed by *Chambers*
Classified Document Master Control Station, NASA
Scientific and Technical Information Facility

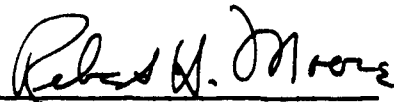
AVAILABLE [REDACTED]

UNCLASSIFIED

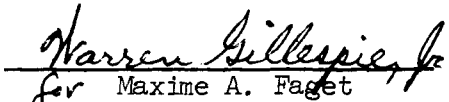

NASA Program Apollo Working Paper No. 1137

STATIC AND DYNAMIC STABILITY CHARACTERISTICS OF THE
APOLLO LEV CANARD-POST ABORT CONFIGURATION

Prepared by:


Robert H. Moore
ASTD, Aerodynamics Branch

Authorized for Distribution:


for Maxime A. Faget
Assistant Director for
Engineering and Development

NATIONAL AERONAUTICS AND SPACE ADMINISTRATION

MANNED SPACECRAFT CENTER

Houston, Texas


September 14, 1964


TABLE OF CONTENTS

Section	Page
SUMMARY	1
INTRODUCTION	1
SYMBOLS	2
MODELS AND TEST FACILITIES	3
Static Stability Tests	4
Dynamic Stability Tests	4
PRESENTATION OF RESULTS	4
DISCUSSION	5
Static Stability Data	5
Dynamic Stability Data	5
CONCLUSIONS	6
TABLE 1	8
FIGURES	9

LIST OF FIGURES

Figure		Page
1	Sketch showing body axis system used	9
2	Sketch of the Apollo Launch Escape Vehicle configuration tested showing general dimensions. (All dimensions in inches)	10
3	Photographs of configuration tested	
	(a) Configuration mounted in JPL 20-inch tunnel . . .	11
	(b) Plan view of canard nose section tested on configuration at Ames facilities	12
	(c) Head on view of canard nose section tested on configuration at Ames facilities	13
4	Aerodynamic characteristics of the Apollo Launch Escape Vehicle without the proposed post-abort canard surfaces at Mach number 0.50 to 1.30	
	(a) Pitching-moment coefficient	14
	(b) Normal-force coefficient	15
	(c) Axial-force coefficient	16
5	Aerodynamic characteristics of the Apollo Launch Escape Vehicle with the proposed post-abort canard surfaces at Mach number 0.50 to 3.40	
	(a) Pitching-moment coefficient	17
	(b) Normal-force coefficient	18
	(c) Axial-force coefficient	19
6	Aerodynamic characteristics of the Apollo Launch Escape Vehicle with the proposed post-abort canard surfaces at Mach number 2.00 to 7.30	
	(a) Pitching-moment coefficient	20
	(b) Normal-force coefficient	21
	(c) Axial-force coefficient	22

Figure		Page
7	Schlieren photograph of tests on the Apollo LEV- post abort canard configuration in the Jet Propulsion Laboratory at Mach numbers of 2.0, 3.0, 3.5, 4.0, and 4.75	23
8	Dynamic stability characteristics of the Apollo Launch Escape Vehicle configuration with proposed post-abort canard surfaces at Mach numbers of .3 to 4.5	
	(a) Mach number = .3	26
	(b) Mach number = .5	27
	(c) Mach number = .7	28
	(d) Mach number = 1.5	29
	(e) Mach number = 2.0	30
	(f) Mach number = 3.0	31
	(g) Mach number = 4.5	32

[REDACTED]

STATIC AND DYNAMIC STABILITY CHARACTERISTICS OF THE
APOLLO LEV CANARD-POST ABORT CONFIGURATION

SUMMARY

A preliminary investigation at Mach numbers from 0.5 to 7.3 has been conducted in the Ames Unitary wind tunnels and the Jet Propulsion Laboratory 20-inch and 21-inch tunnels on the Apollo LEV Canard-Post Abort configuration to determine the static stability characteristics of the configuration. Also, a dynamic stability investigation at Mach numbers from 0.16 to 4.5 has been conducted in the Jet Propulsion Laboratory 20-inch tunnel and the Langley 20-foot free-spinning tunnel.

The pitching-moment data indicate that for the data reduction center of gravity used the canard surfaces eliminate the apex forward trim point for all Mach numbers up to about 5.2. It should be noted that the trim point is very dependent on center-of-gravity location. At a Mach number of 5.2 the configuration has a static trim point at an angle-of-attack of about 12° . It is believed the presence of this trim point is due to a severe shock interaction phenomenon acting on the command module.

Data from the dynamic stability tests indicates the configuration to be stable in the heat shield forward position for all the Mach numbers tested; ~~however, the configuration did have a limit oscillation of about $\pm 20^\circ$ at the subsonic Mach numbers tested.~~

INTRODUCTION

The initial Apollo launch escape vehicle configuration and the Apollo command module alone configuration have been tested at several facilities; the Ames Research Center, Arnold Engineering and Development Center, Jet Propulsion Laboratory, North American Aviation, and the Langley Research Center. The purpose of those tests was to determine the aerodynamic characteristics of the Apollo configurations for use in studies of the Apollo missions. The results of these indicate the command module alone configuration to have a secondary trim point (apex forward). This secondary trim point exists throughout the Mach numbers range tested. Analysis of trajectory studies indicates this secondary trim point to be a serious problem in the event of an aborted flight. The major problem in the event of an abort with this secondary trim point is due to the excess dynamic pressure build-up and the associated high accelerations encountered on high altitude abort. The apex cover cannot be jettisoned; for the deployment of the recovery system, due to the

[REDACTED]

excessive dynamic pressure. Therefore, the prime contractor was requested to study modifications designed to eliminate this secondary trim point.

At about this same point in the program, personnel of the Aerodynamics Branch, Manned Spacecraft Center, Houston, Texas, proposed a configuration with deployable canard surfaces mounted at/or near the apex of the rocket motor nose. These canard surfaces would be an integral part of the rocket motor nose section and would be deployed only in the event of an abort. The Manned Spacecraft Center was given the responsibility of developing the post-abort canard configuration. An analytical study indicated that canard surfaces of five square feet (per canard) would be sufficient to fulfill the required mission.

In the event of an abort the launch escape rocket would fire at time zero and propel the launch escape vehicle away from the booster. At $t = 8$ seconds, the launch escape rocket burns out. At $t = 11$ seconds, the canard surfaces would be deployed utilizing a pyrotechnic actuator. A canard deployment time of approximately $\frac{1}{4}$ -second is anticipated. At altitudes below 25,000 feet, the tower-rocket apex cover combination is jettisoned at $t = 14$ seconds. The drogue parachute is deployed for normal recovery using the clustered-parachute system at $t = 16$ seconds. For altitudes above 25,000 feet and below 120,000 feet, the launch escape system (tower-rocket combination) is retained until an altitude of 25,000 feet is reached, at which time the tower-rocket-apex cover combination is jettisoned and the normal recovery sequence initiated. Above 120,000 feet, the launch escape system (tower-rocket combination) is manually jettisoned by the pilot at approximately 10 to 15 seconds after abort initiation and the C/M rate damping mode initiated. The pilot manually orients the vehicle to a heat shield forward position and the normal entry recovery sequence is then initiated when the spacecraft reaches 25,000 feet.

Static and dynamic force tests have been conducted in the Ames Unitary wind tunnels, the Jet Propulsion Laboratory 20-inch and 21-inch tunnels, and the Langley 20-foot free-spinning tunnel through a Mach number range from about 0.16 to 7.3. The purpose of this paper is to report the results of these tests.

SYMBOLS

Data are presented using the body system of axes shown in figure 1. The symbols and coefficients used in this paper are defined as follows.

C_M	pitching-moment coefficient, $\frac{\text{pitching-moment}}{q SD}$
C_N	normal-force coefficient, $\frac{\text{normal force}}{q S}$
C_A	axial-force coefficient, $\frac{\text{axial-force}}{q S}$
C_{m_q}	$\left(\frac{d C_m}{d \frac{qD}{2V}} \right)$
$C_{m_{\dot{\alpha}}}$	$\left(\frac{d C_m}{d \frac{\dot{\alpha}D}{2W}} \right)$
q	dynamic pressure, lb/sq ft
$\dot{\alpha}$	rate of change of angle-of-attack, d/dt
V	free-stream velocity, ft/sec
D	reference dimension (command module diameter), ft
M	free-stream Mach number
S	reference area D^2 , sq ft
α	angle-of-attack of model center line, deg
$\frac{X}{D}$	longitudinal location of the center-of-gravity from theoretical command module apex
$\frac{Z}{D}$	vertical location of center-of-gravity relative to center line

MODELS AND TEST FACILITIES

General dimensions of the Apollo Launch Escape Vehicle configuration tested in the different facilities are given in figure 2. The model used in the Ames unitary tunnels was a 0.105 scale model (16.2 inch diameter) of the Apollo LEV configuration which is made of stainless steel and aluminum and was modified for the post-abort canard configuration. The two models used at the Jet Propulsion Laboratory facilities were a

[REDACTED]

0.0195-scale model (3 inch diameter) and a 0.0128-scale (2-inch diameter). One was made of stainless steel and aluminum and the other model was made of wood with brass tower and wood rocket motor. The model used in the Langley 20-foot free-spinning tunnel was made of fiberglass with brass tower structure and wood rocket motors and was a 0.0357-scale model (5.5 inch diameter). Photographs of the configuration tested are presented in figure 3.

Test conditions for the various models are summarized in table I. The Reynolds numbers given are based on model maximum diameter.

Static Stability Tests

The static stability tests were conducted in the Ames unitary wind tunnels at Mach numbers from 0.5 to 3.4 and an angle-of-attack range from -40° to 150° and in the Jet Propulsion Laboratory facilities at Mach numbers from 2.0 to 7.3 and an angle-of-attack range of about $\pm 140^\circ$.

Dynamic Stability Tests

The dynamic stability tests were conducted in the JPL 20-inch tunnel at Mach numbers from 0.5 to 4.5 and the tests in the spin tunnel were conducted at a Mach number of about 0.16.

The tests in the JPL 20-inch tunnel were made with the model mounted on a transverse rod which is mounted on a yoke support in the tunnel and the model is free to tumble. The transverse rod passes through the center-of-gravity. The model is restrained in the apex forward position and then released. Analysis of the ensuing motion yields the dynamic stability parameter.

The model used in the spin tunnel tests was a free flight model with the weight, moments of inertia, and center-of-gravity location properly scaled. The model was hand launched into the tunnel and was held in the tunnel by adjusting the speed of the air flow as the spin tunnel is a vertical tunnel.

All of the dynamic stability data was recorded in movie film.

PRESENTATION OF RESULTS

The basic data for the Apollo Launch Escape Vehicle configuration without the proposed post-abort canard surfaces are presented in figure 4 and the data for the configuration with the post-abort canard surfaces, are presented in figures 5 and 6.

[REDACTED]

The static stability data were run at Mach numbers from 0.5 to 7.3, and the dynamic stability data (fig. 8) were run at Mach numbers from about 0.16 to 4.5.

DISCUSSION

Static Stability Data

The basic moment data for the Apollo LEV-canard post-abort configuration were obtained at Mach numbers from 0.5 to 7.3. The angles-of-attack investigated were from -150° to 150° .

The data (figs. 5 and 6) show that the configuration eliminates the apex forward trim point up to about $M = 5.2$. At Mach number 5.2, the configuration has a static trimpoint at an angle-of-attack of about 12° , and at Mach numbers greater than 5.2; the configuration becomes more stable. It should be noted that the trim Mach number and angle-of-attack is very dependent on the model center-of-gravity location. The data show a trend toward an apex forward trim point as early as about Mach 3.0. The explanation for the presence of the trim point has been determined from schlieren photographs (fig. 7) to be due to a severe shock interaction phenomenon acting on the command module. The trim condition becomes progressively more severe with increasing Mach number due to the sweep back angle of the rocket nose and canard shocks. When flow passes through the oblique shock of the rocket and command module section, the total pressure of the flow behind this shock is not severely dropped, while the Mach number is reduced considerably. When this high total pressure behind the oblique shock is stagnated or near stagnated through a normal shock existing in the command module at angles-of-attack of about 15° , the total pressure loss through this normal shock is much less due to the lower Mach number flow. Therefore, the command module will have pressures which are very large, and pressure coefficients as high as 3.5 exist. These pressure coefficient values are two times as great as would be expected when flow stagnates through a normal shock of free-stream condition. All of these loads are applied aft of the center-of-gravity location and contribute a large restoring moment. Also the pitching-moment coefficient is increased by a factor of about 1.5 to 2.0 over the "clean" Apollo Launch Escape Vehicle configuration.

Dynamic Stability Data

The Apollo LEV-canard post-abort configuration was tested in the Langley 20-foot free-spinning tunnel and the JPL 20-inch tunnel at a Mach number range from about 0.16 to 4.5.

As the only way the dynamic data was recorded in the spin tunnel was by movie camera and visual observation, the observation is best reported. The model was hand launched into the spin tunnel and was in free-fall all the time, until the model was let down into the retrieving net for recovery from the tunnel. The model was launched with the apex forward into the flow and, as soon as the model was released, it would turn around heat-shield forward. In the heat shield forward position the model oscillated about the center-of-gravity location and also had a rotation rate about the axis of symmetry. The angle of oscillation is estimated to be about $\pm 25^\circ$ to 30° and the rate of rotation is about 0.05 revolutions per second (full scale value). The configuration was launched without the canard surfaces and it trimmed out at about $\alpha = 5^\circ$ (apex forward).

The model used in the dynamic stability tests in the JPL facility was mounted in a transverse rod with ball bearings; (the transverse rod passes through the center-of-gravity location) and was held in the apex forward position (apex pointed into the air flow) with a braking system. The model was free to rotate 360° . The configuration was released from several different angles-of-attack and the model motions were recorded by high speed movie cameras.

The movie films were then read to obtain position-time histories of the model motions. Values of $C_{m_q} + C_{m_{\dot{\alpha}}}$ as a function of oscillation amplitude can be obtained from analysis of the position-time history.

For use in present computer programs, the damping derivatives must be expressed as a function of angle-of-attack. This is accomplished by modifying the shape of the $C_{m_q} + C_{m_{\dot{\alpha}}}$ versus oscillation amplitude curve. These values are then put into a single degree of freedom computer program where a derived motion is obtained for comparison with the measured position time histories.

*See
c/124921*
The dynamic tests indicated the configuration to be stable in the heat-shield forward position throughout the Mach number range tested. At Mach numbers of 0.30, 0.50, and 0.70 the configuration indicated a limit cycle of about $\pm 20^\circ$.

CONCLUSIONS

The results of stability tests of the Apollo-LEV post-abort configuration indicated the following conclusions.

1. For the data reduction center of gravity used, the post-abort canard surfaces eliminated the apex forward trim point at all Mach numbers up to 5.2. At $M = 5.2$ and for all Mach numbers tested above $M = 5.2$, the configuration has a static trim point at an angle of attack of about 12° .

2. The presence of this apex forward trim point is believed to be due to a severe shock interaction phenomenon.

3. The configuration is dynamically stable in the heat shield forward position for all Mach numbers tested, ~~however, at the subsonic Mach numbers the configuration did have a limit oscillation of about $\pm 20^\circ$.~~

TABLE I. - TEST CONDITIONS

Facility	Purpose	Model scale	Reynolds no. range ¹	M-Range	Range
Ames 11'	Static	0.105	$3.4 - 6.5 \times 10^6$	0.5 to 1.2	-40° to +160°
9 x 7	Static	0.105	$3.3 - 3.6 \times 10^6$	1.65 and 2.00	-40° to +160°
8 x 7	Static	0.105	$3.8 - 4.2 \times 10^6$	3.00 and 3.40	-40° to +160°
JPL 20-inch	Static	0.0195	$3.7 - 6.8 \times 10^6$	2.00 and 4.76	-50° to +130°
	Dynamic	0.0195	.086 - 7.8×10^6	0.30 to 4.50	free to tumble
21 inch	Static	0.0195	6.5×10^6	5.50 to 7.30	-5° to 50°
Langley spin	Dynamic	0.0357	$.163 \times 10^6$.05	free flight

¹Reynolds numbers are based on model maximum diameter.

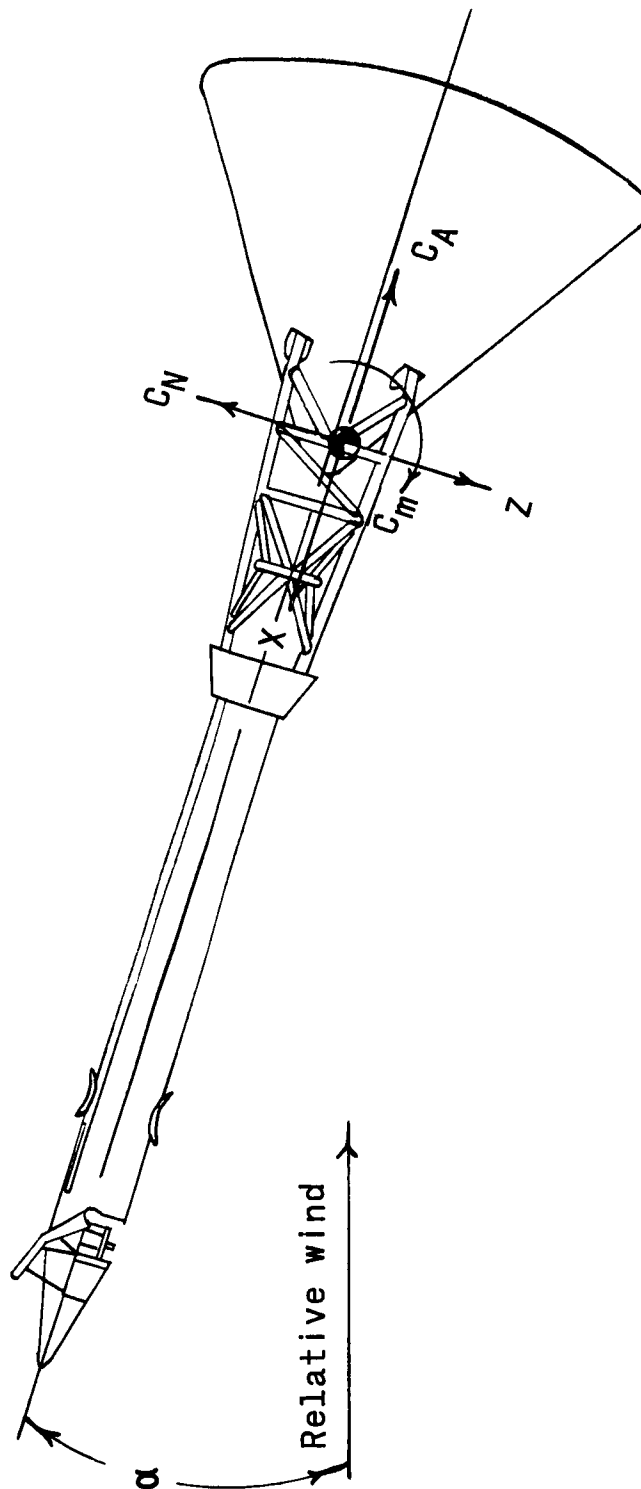


Figure 1.- Sketch showing body axis system used.

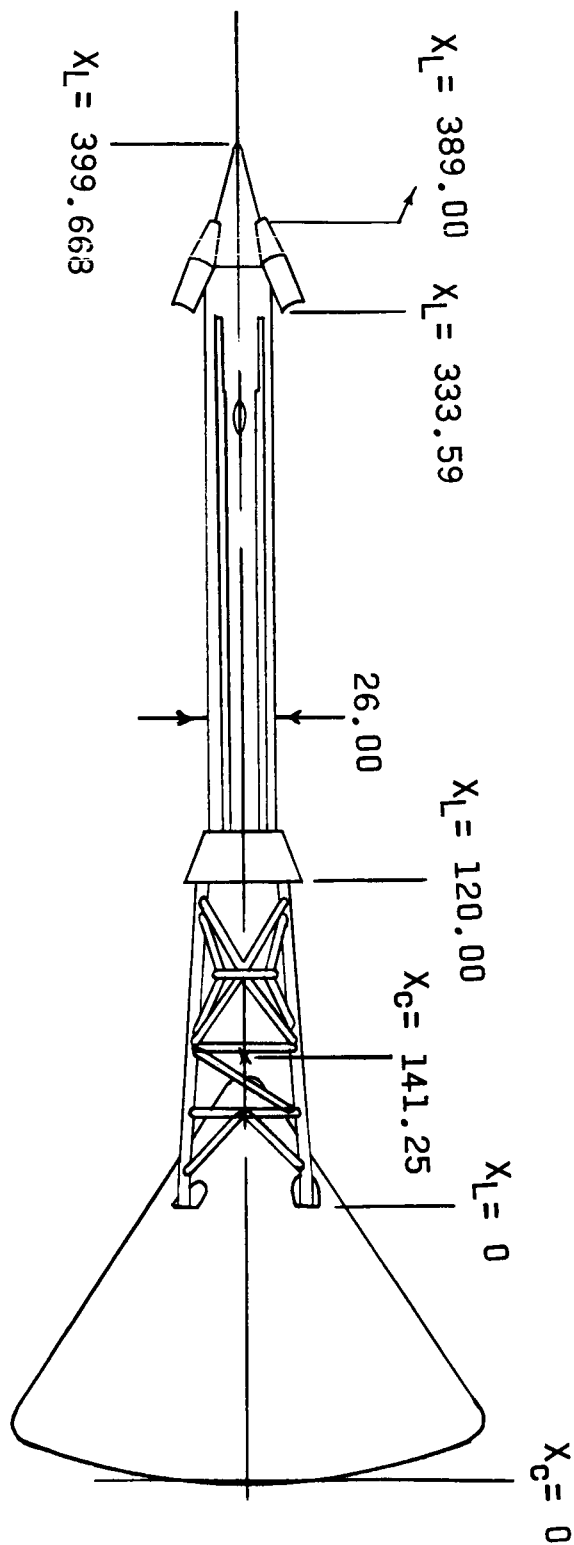
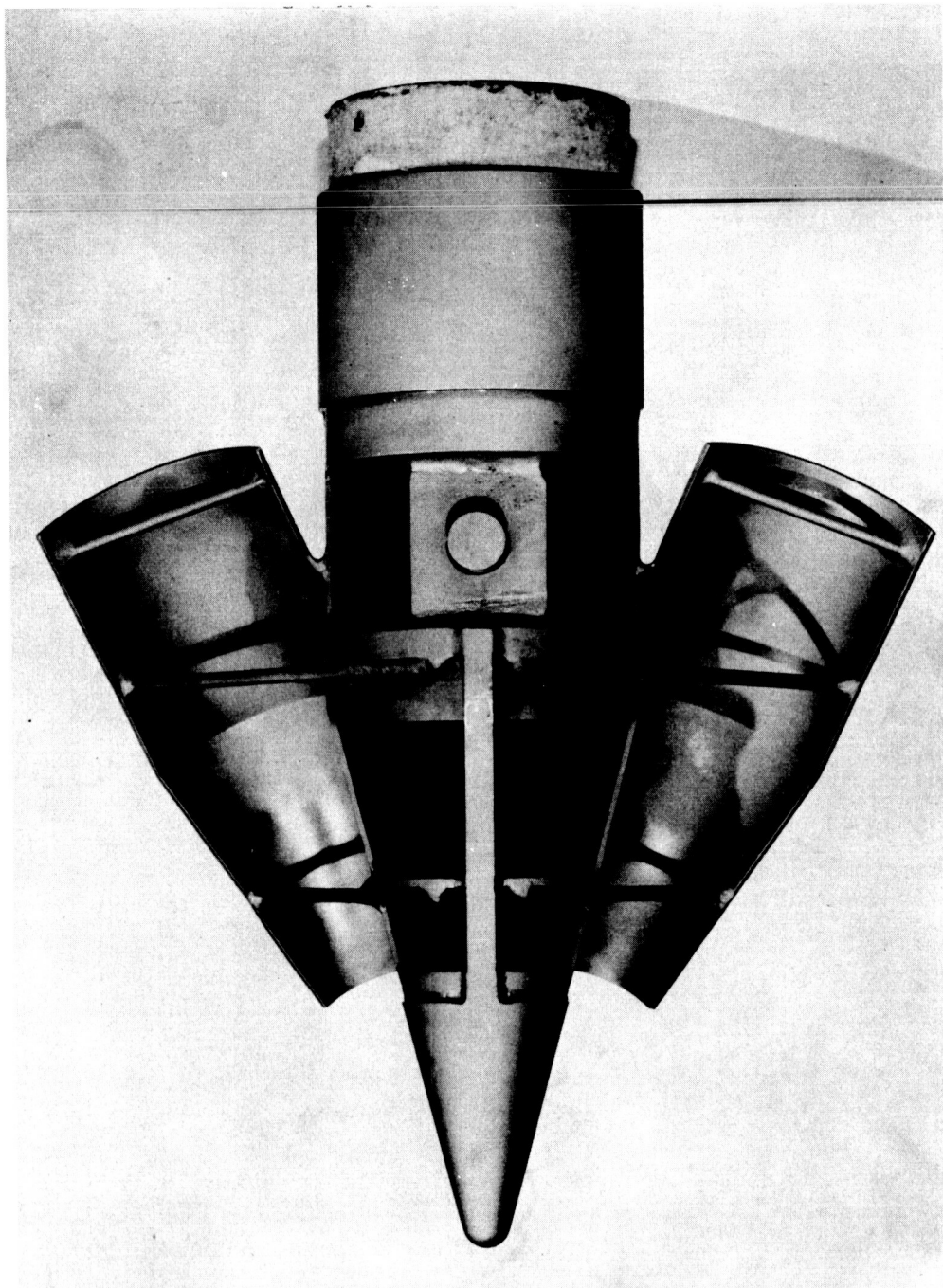


Figure 2.- Sketch of the Apollo Launch Escape Vehicle configuration tested showing general dimensions. (All dimensions in inches).



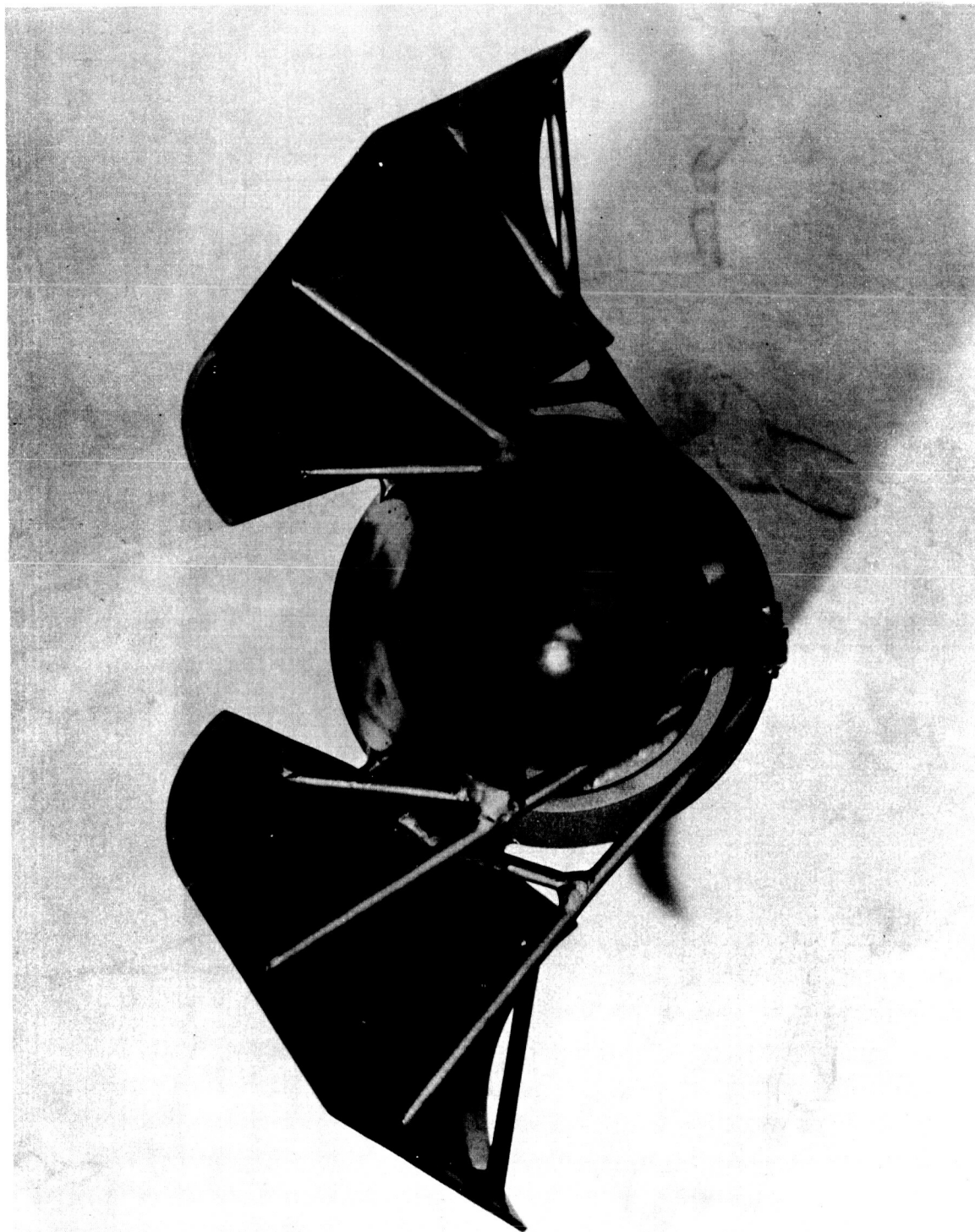
(a) Configuration mounted in JPL 20-inch tunnel.

Figure 3.- Photographs of configuration tested.



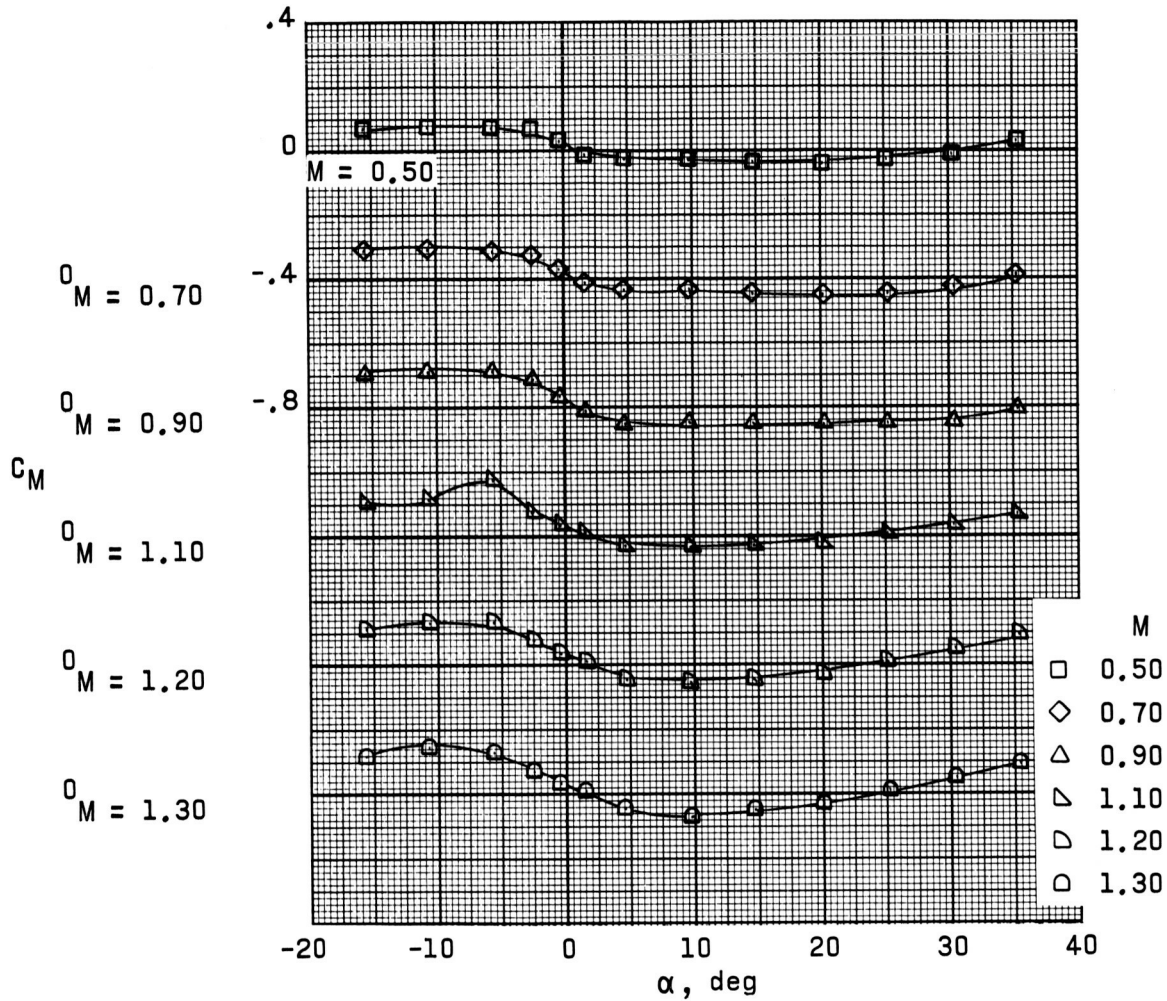
(b) Plan view of canard nose section tested on configuration at Ames facilities.

Figure 3.- Continued.



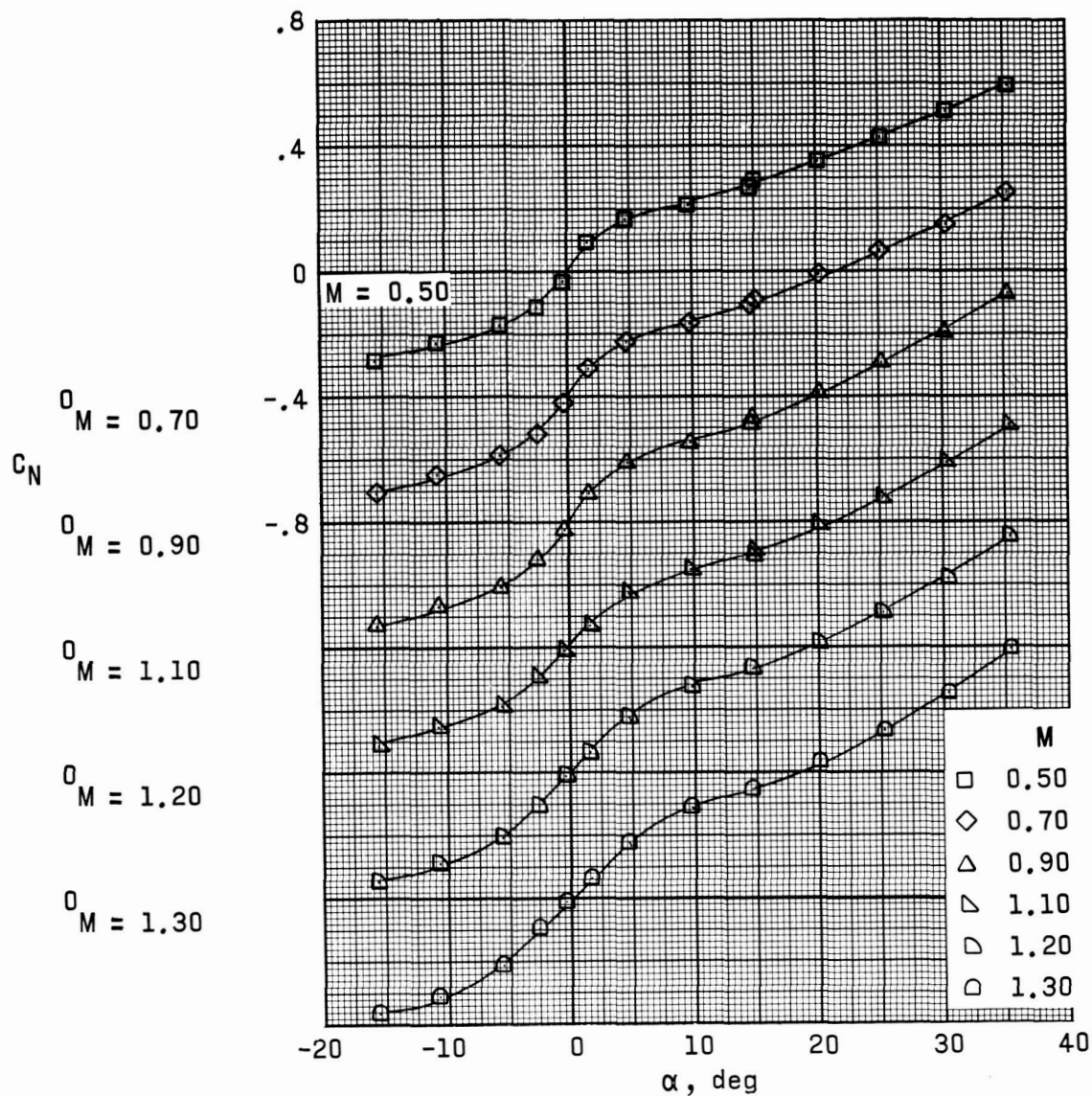
(c) Head on view of canard nose section tested on configuration at Ames facilities.

Figure 3.- Concluded.



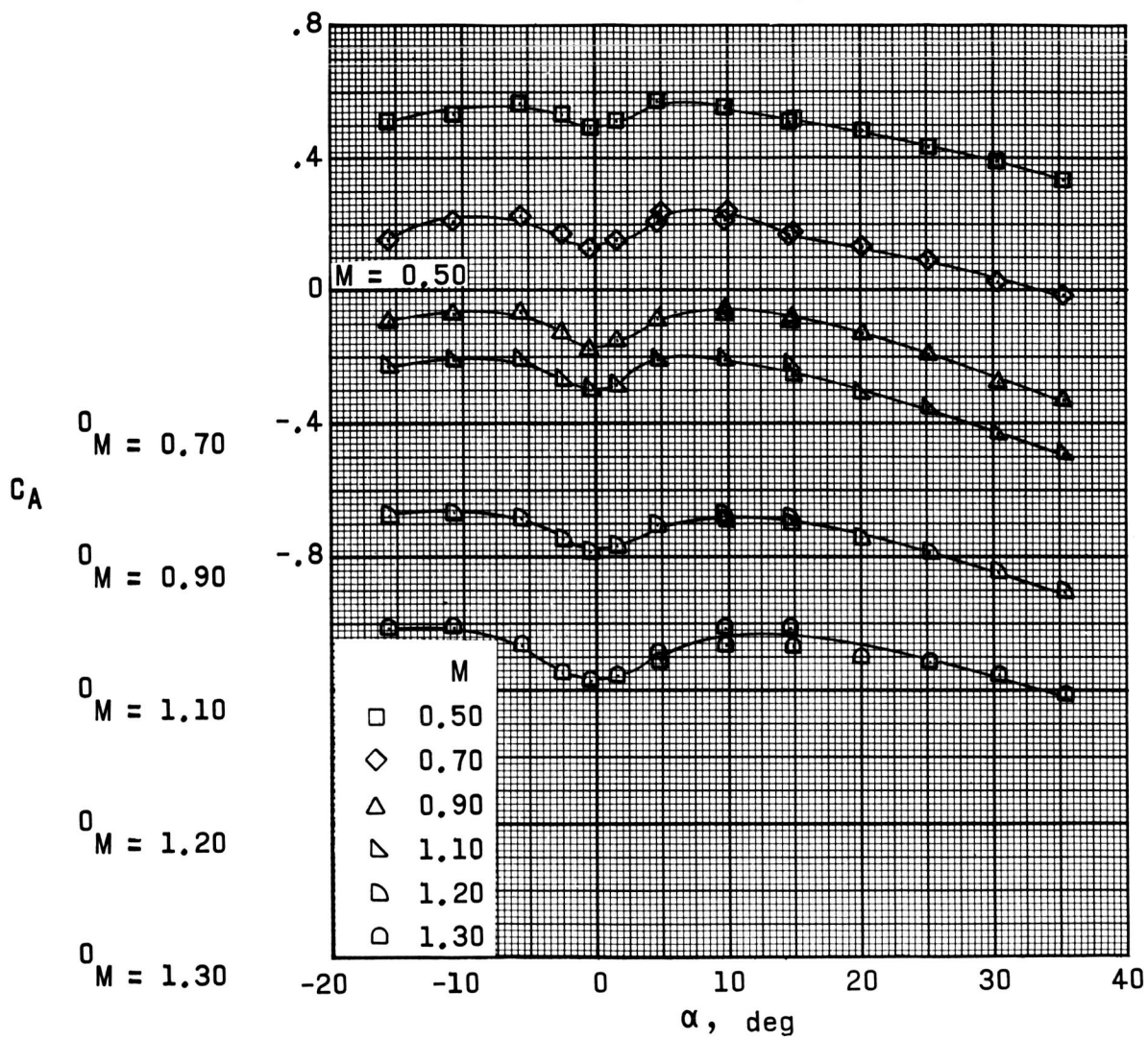
(a) Pitching-moment coefficient.

Figure 4.- Aerodynamic characteristics of the Apollo Launch Escape Vehicle without the proposed post-abort canard surfaces at Mach number 0.50 to 1.30.



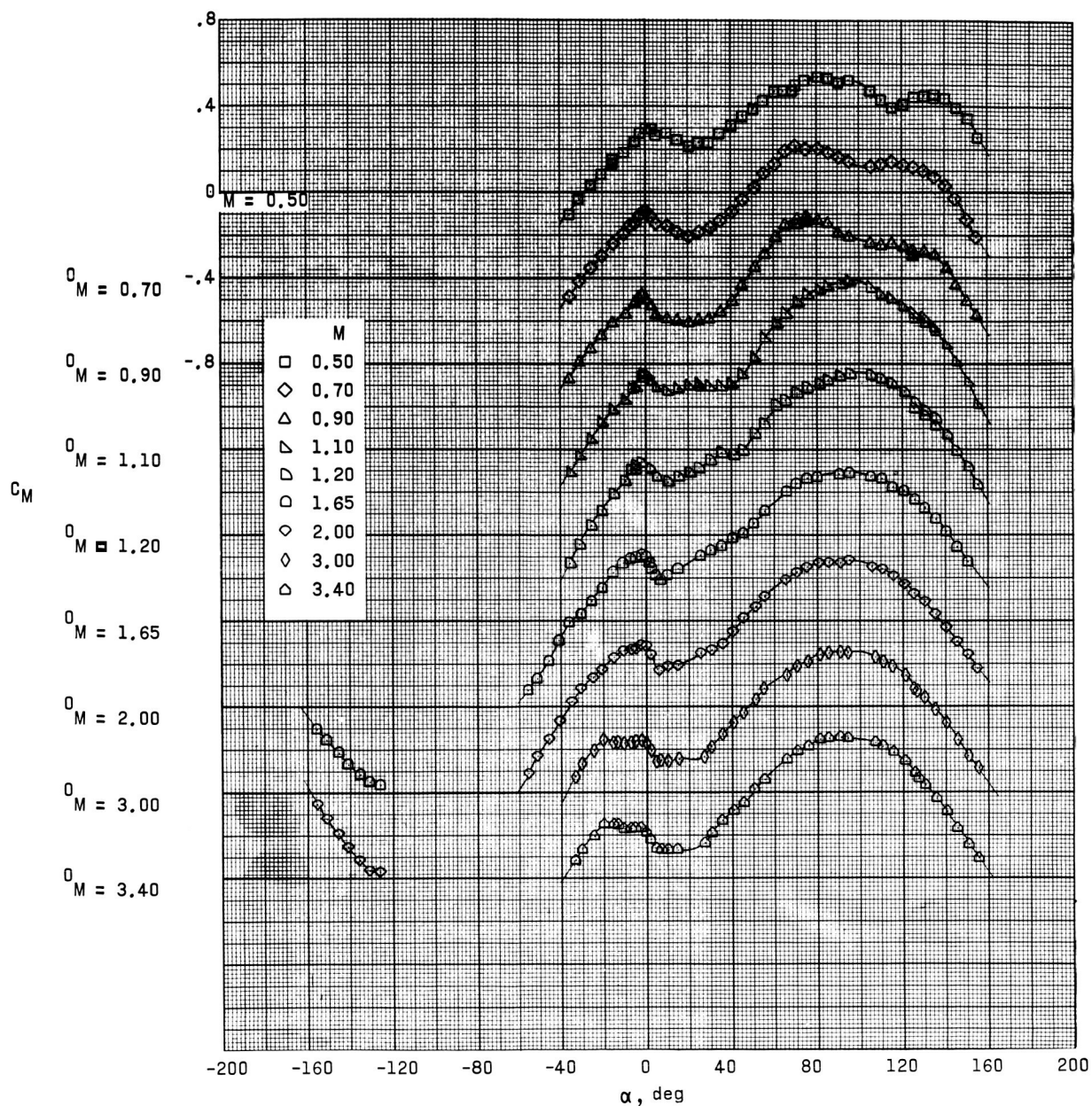
(b) Normal-force coefficient.

Figure 4.- Continued.



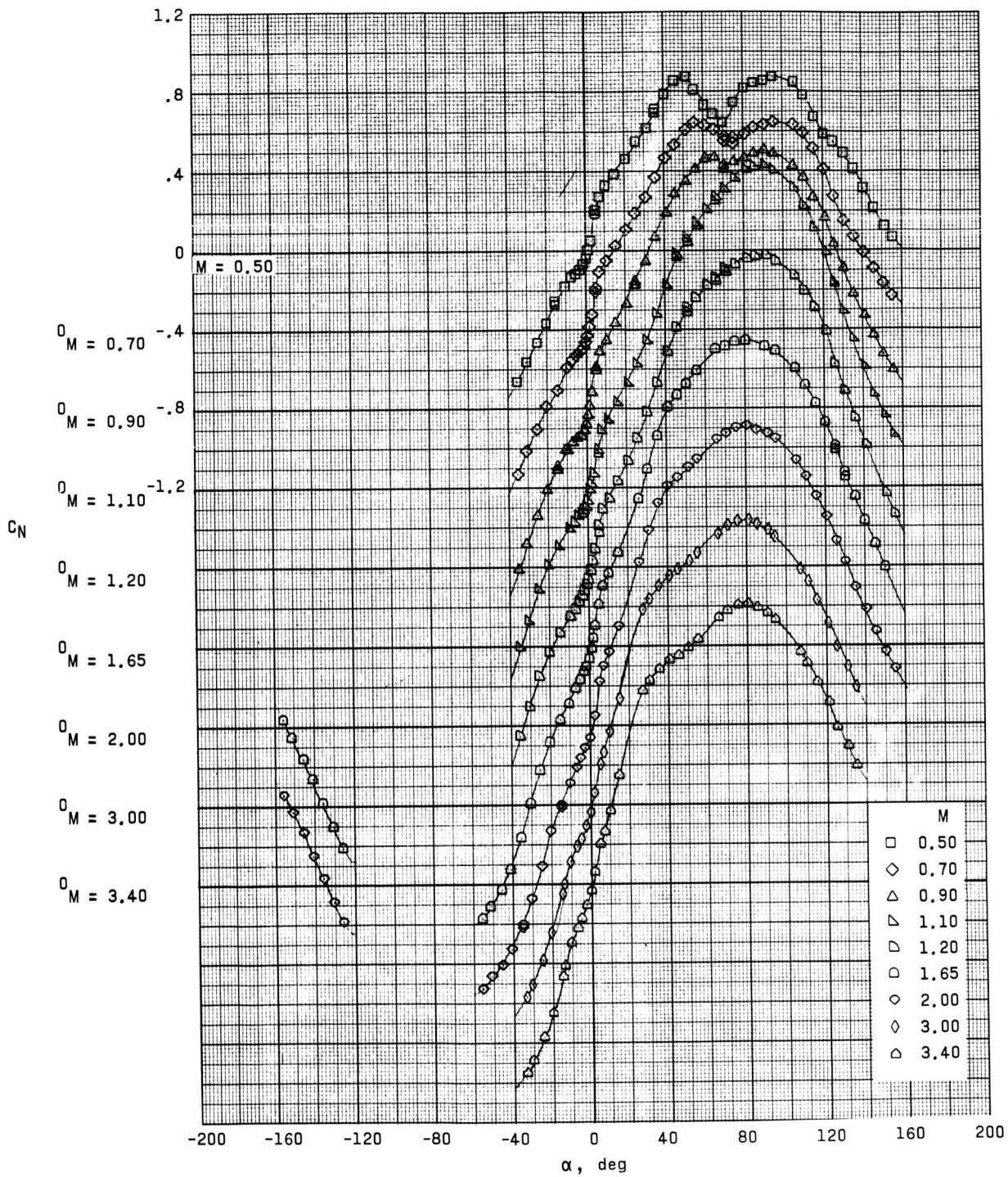
(c) Axial-force coefficient.

Figure 4.- Concluded.



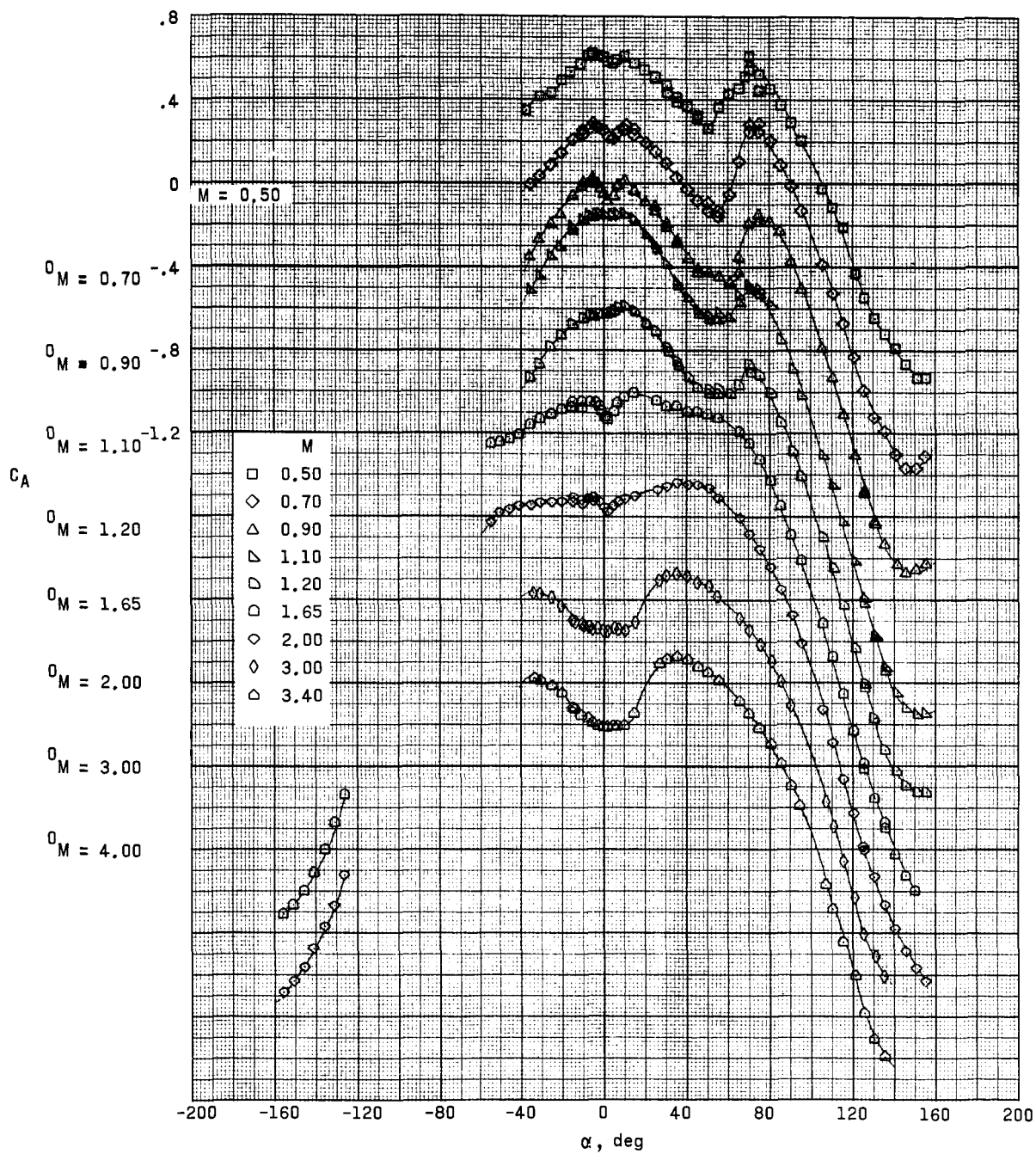
(a) Pitching-moment coefficient.

Figure 5.- Aerodynamic characteristics of the Apollo Launch Escape Vehicle with the proposed post-abort canard surfaces at Mach number 0.50 to 3.40.



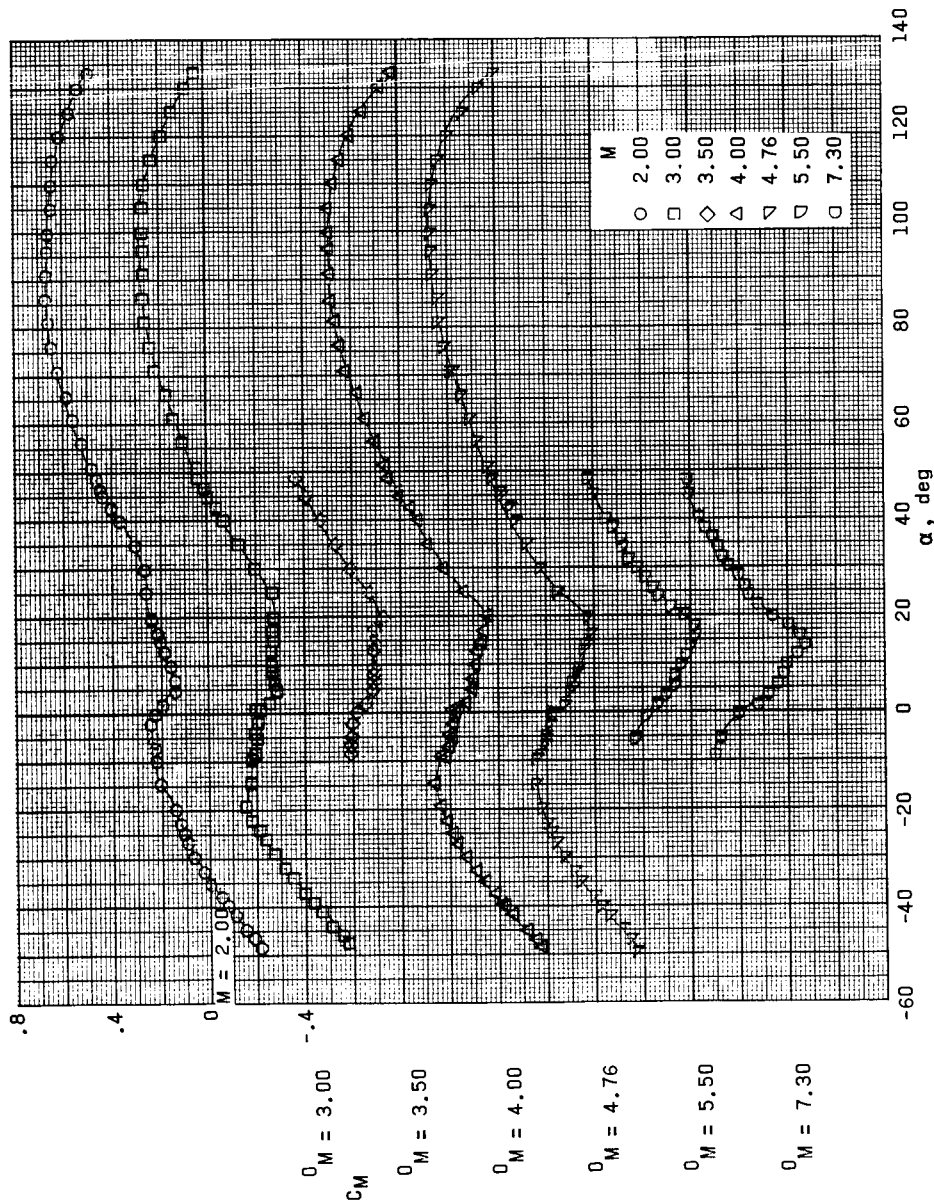
(b) Normal-force coefficient.

Figure 5.- Continued.



(c) Axial-force coefficient.

Figure 5.- Concluded.

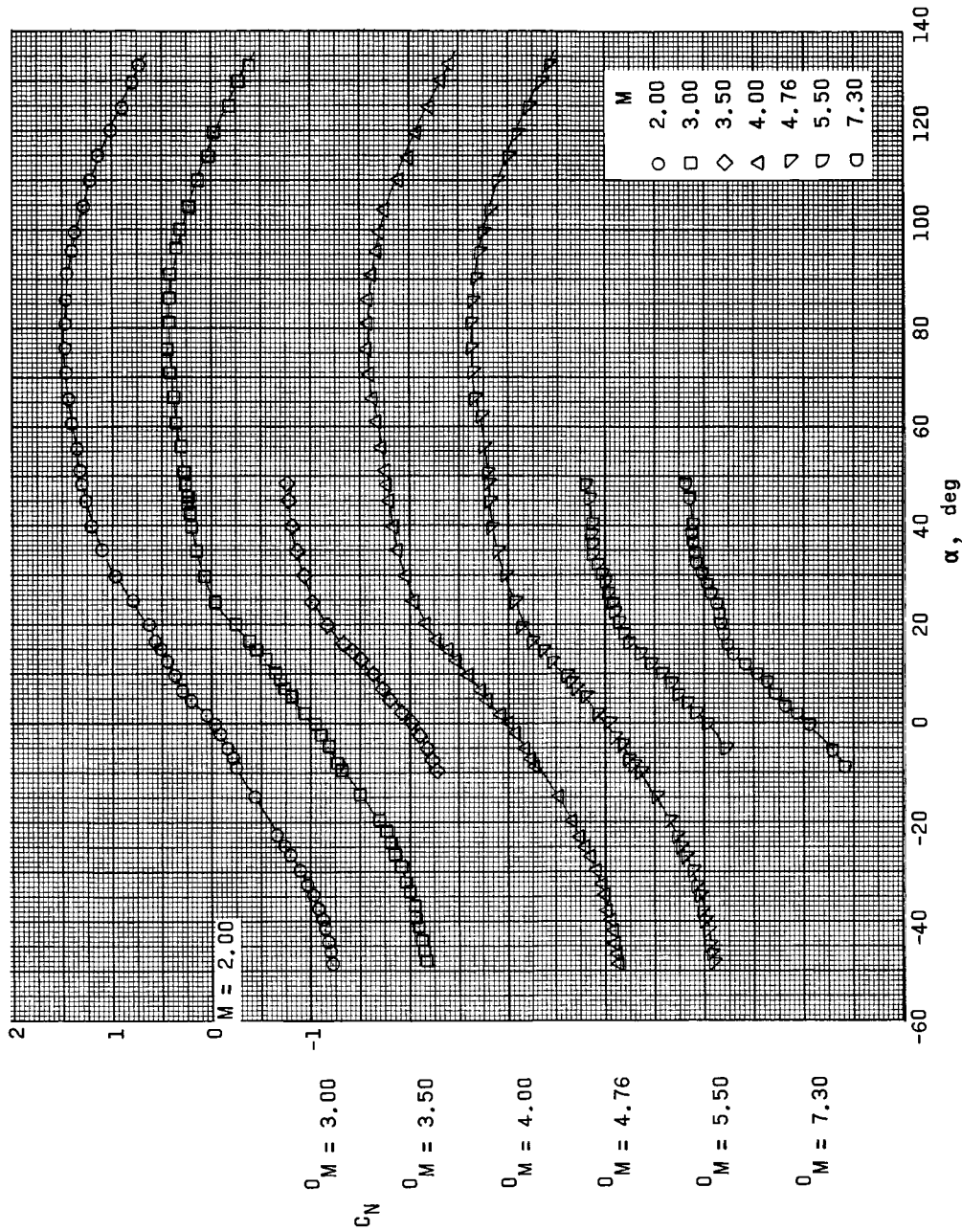


(a) Pitching-moment coefficient.

Figure 6.- Aerodynamic characteristics of the Apollo Launch Escape Vehicle with the proposed post-abort canard surfaces at Mach number 2.00 to 7.30.

CONFIDENTIAL

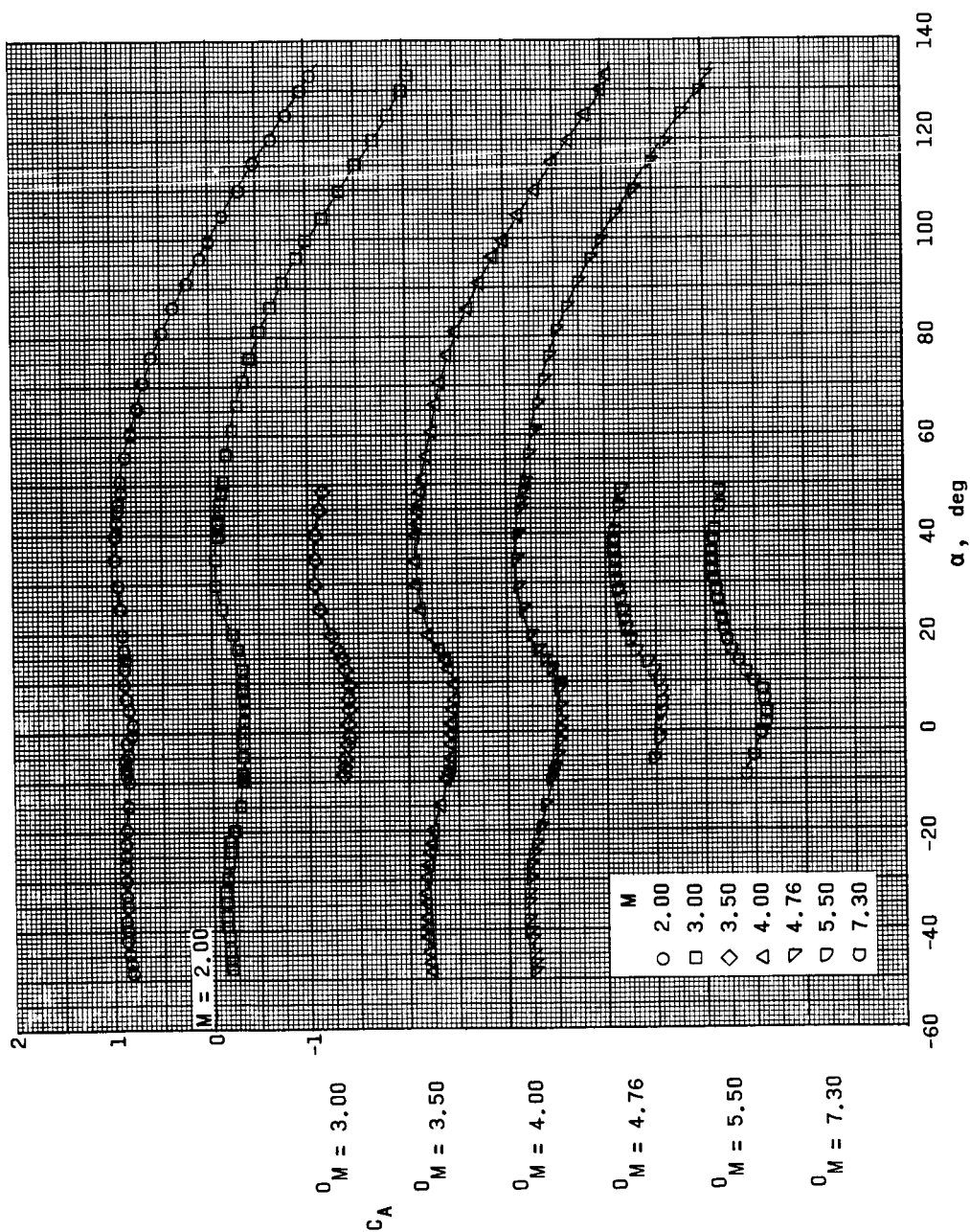
CONFIDENTIAL



(b) Normal-force coefficient.

Figure 6.- Continued.

CONFIDENTIAL



(c) Axial-force coefficient.

Figure 6.- Concluded.



$M = 2.0 \quad \alpha = 0^\circ$



$M = 2.0 \quad \alpha = 20^\circ$



$M = 3.0 \quad \alpha = 0^\circ$



$M = 3.0 \quad \alpha = 20^\circ$

Figure 7.- Schlieren photograph of tests on the Apollo LEV-post abort canard configuration in the Jet Propulsion Laboratory at Mach numbers of 2.0, 3.0, 3.5, 4.0, and 4.75.



$M = 3.5$ $\alpha = 20^\circ$



$M = 4.0$ $\alpha = 20^\circ$



$M = 3.5$ $\alpha = 30^\circ$



$M = 4.0$ $\alpha = 0^\circ$

Figure 7.- Continued.



$M = 4.75$ $\alpha = 20^\circ$

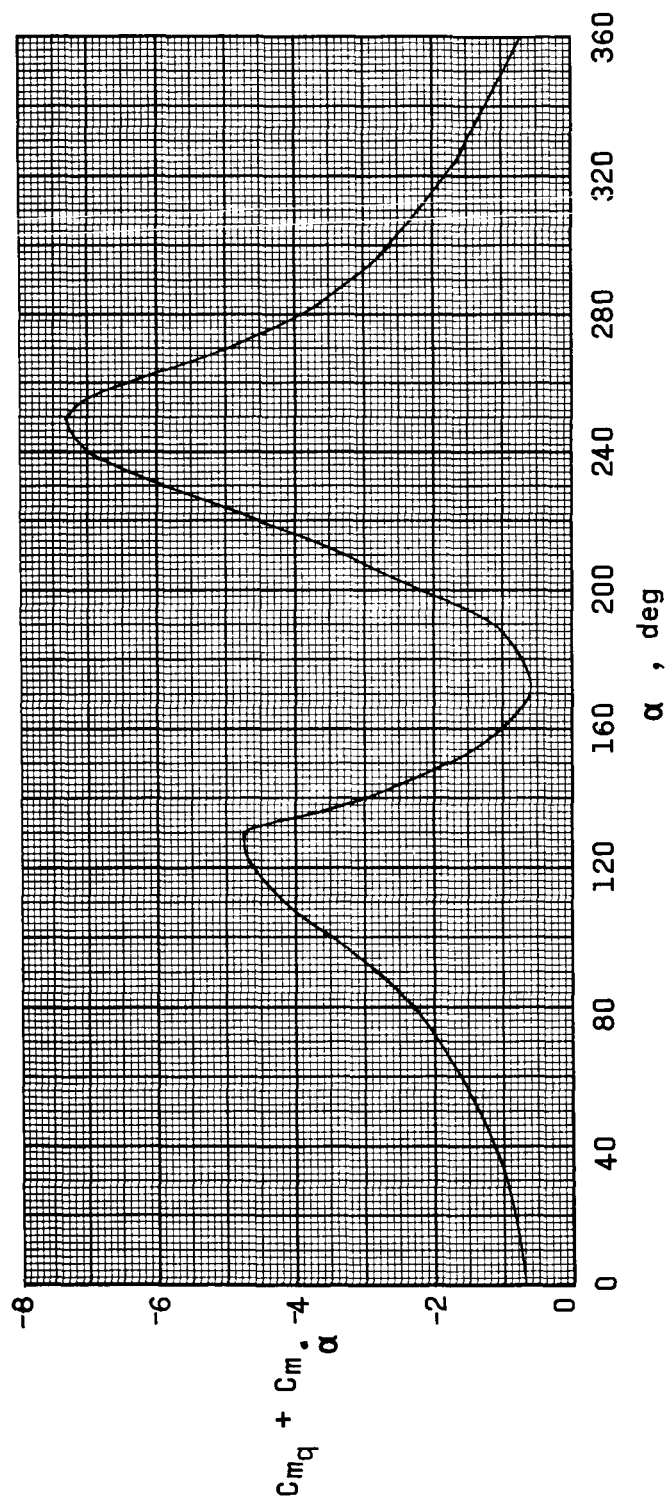
$M = 4.75$
 $\alpha = 20^\circ$
 $\phi_{\text{sting}} = 90^\circ$



$M = 4.75$ $\alpha = 0^\circ$

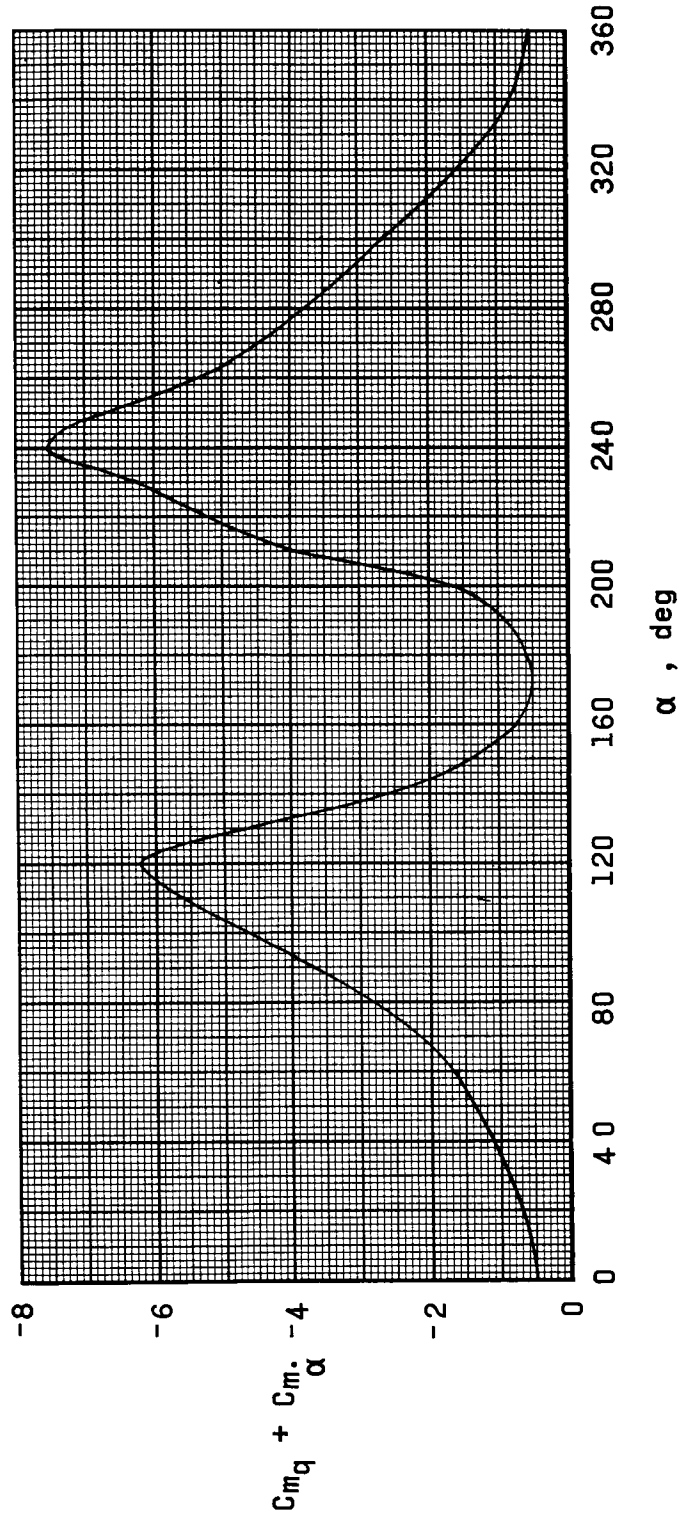


Figure 7.- Concluded.



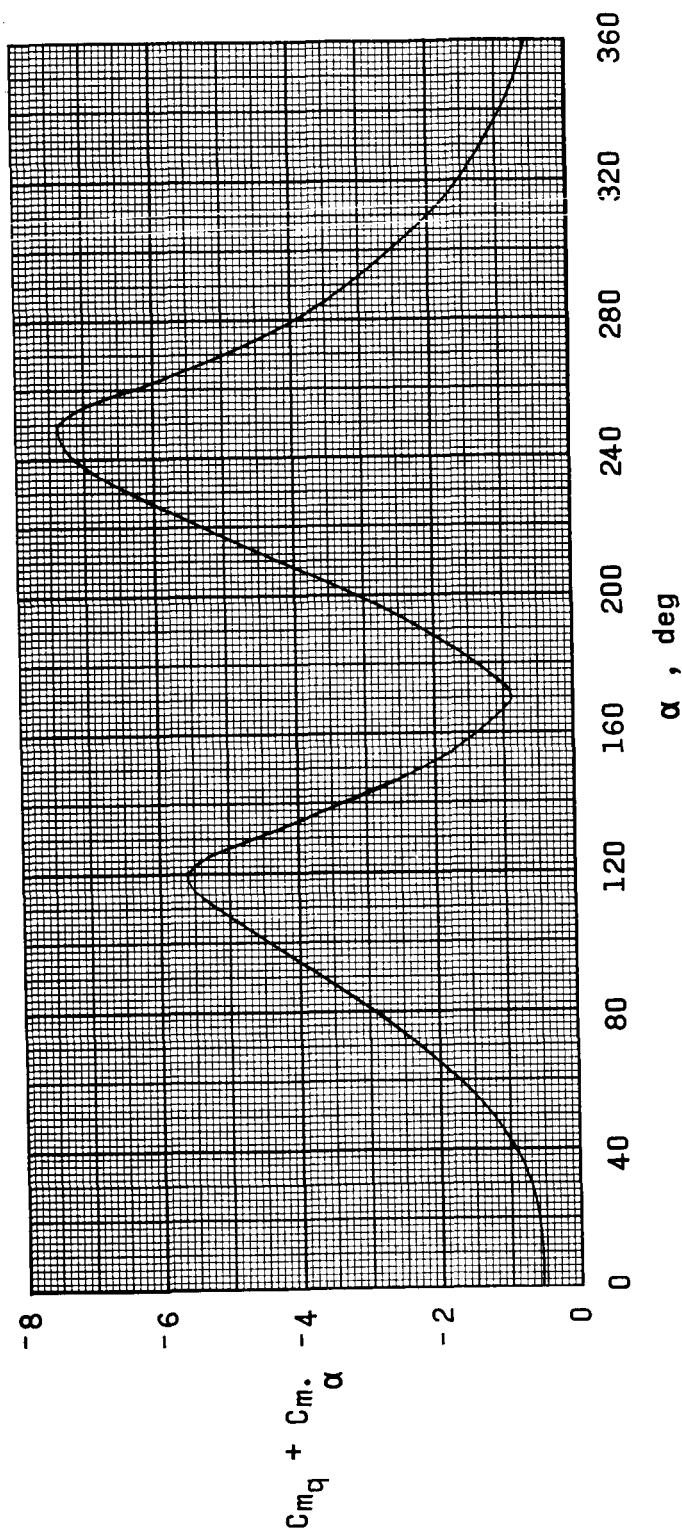
(a) Mach number = .3.

Figure 8.- Dynamic stability characteristics of the Apollo Launch Escape Vehicle configuration with proposed post-abort canard surfaces at Mach numbers of .3 to 4.5.



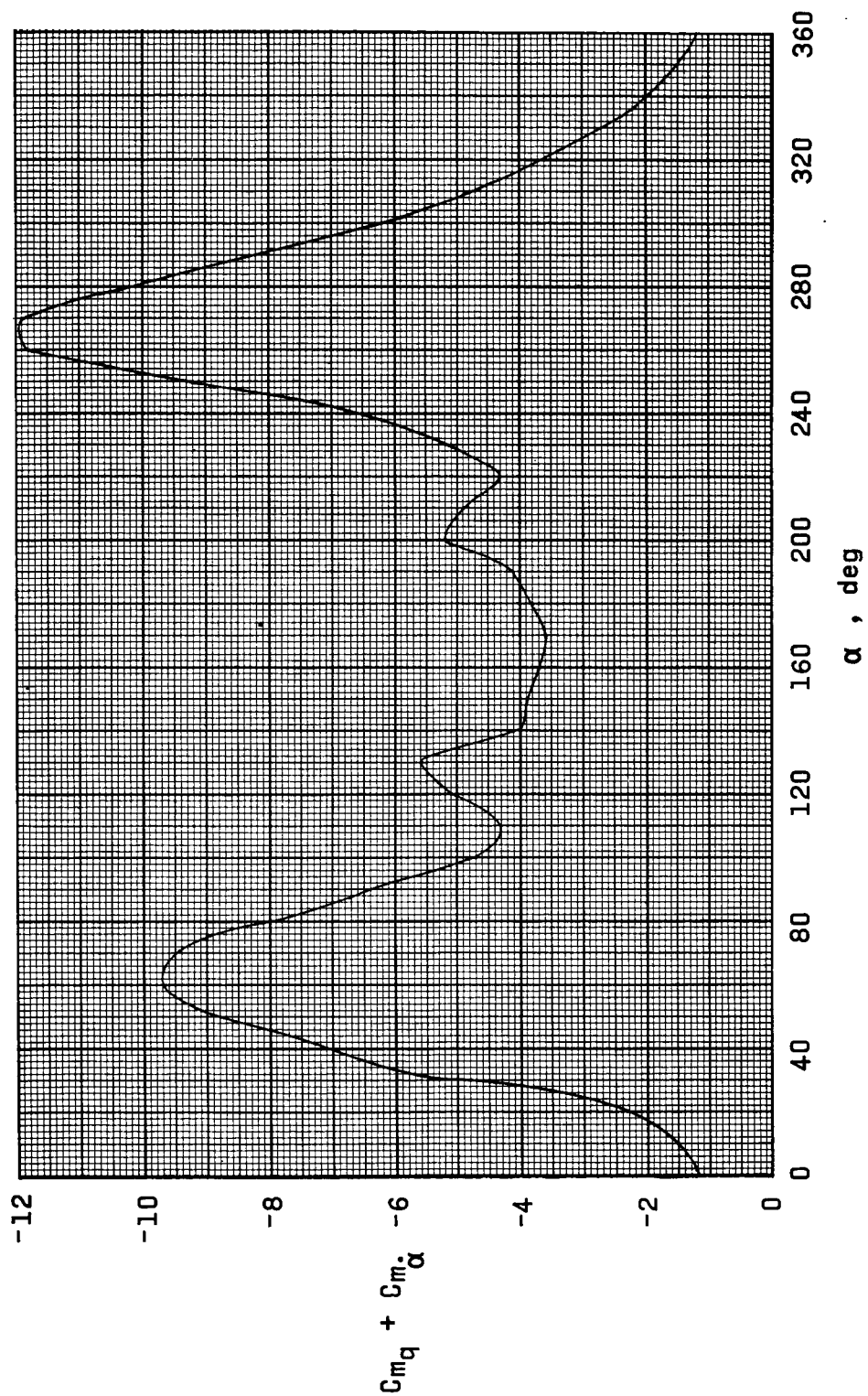
(b) Mach number = .5.

Figure 8.- Continued.



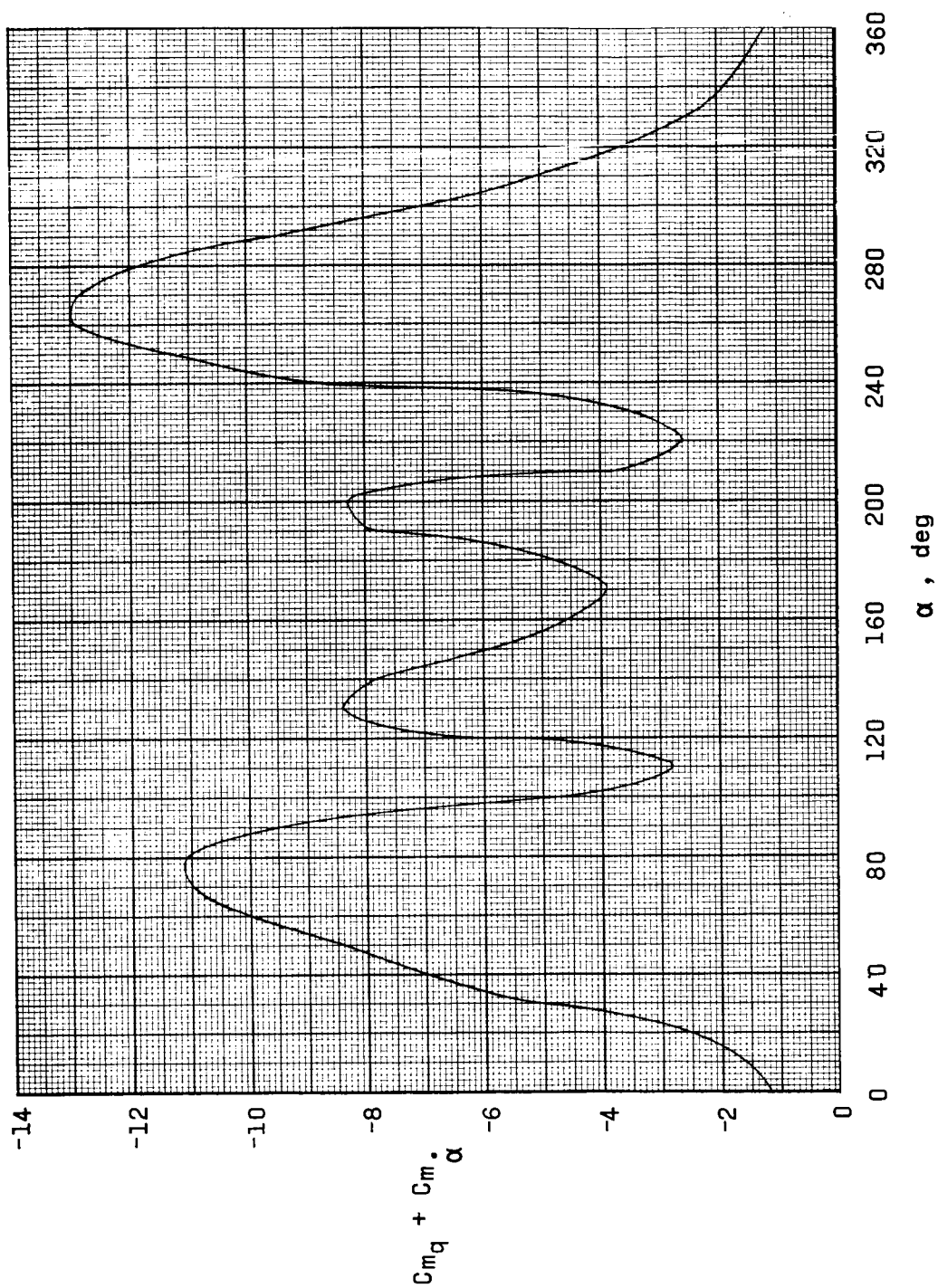
(c) Mach number = .7.

Figure 8.- Continued.



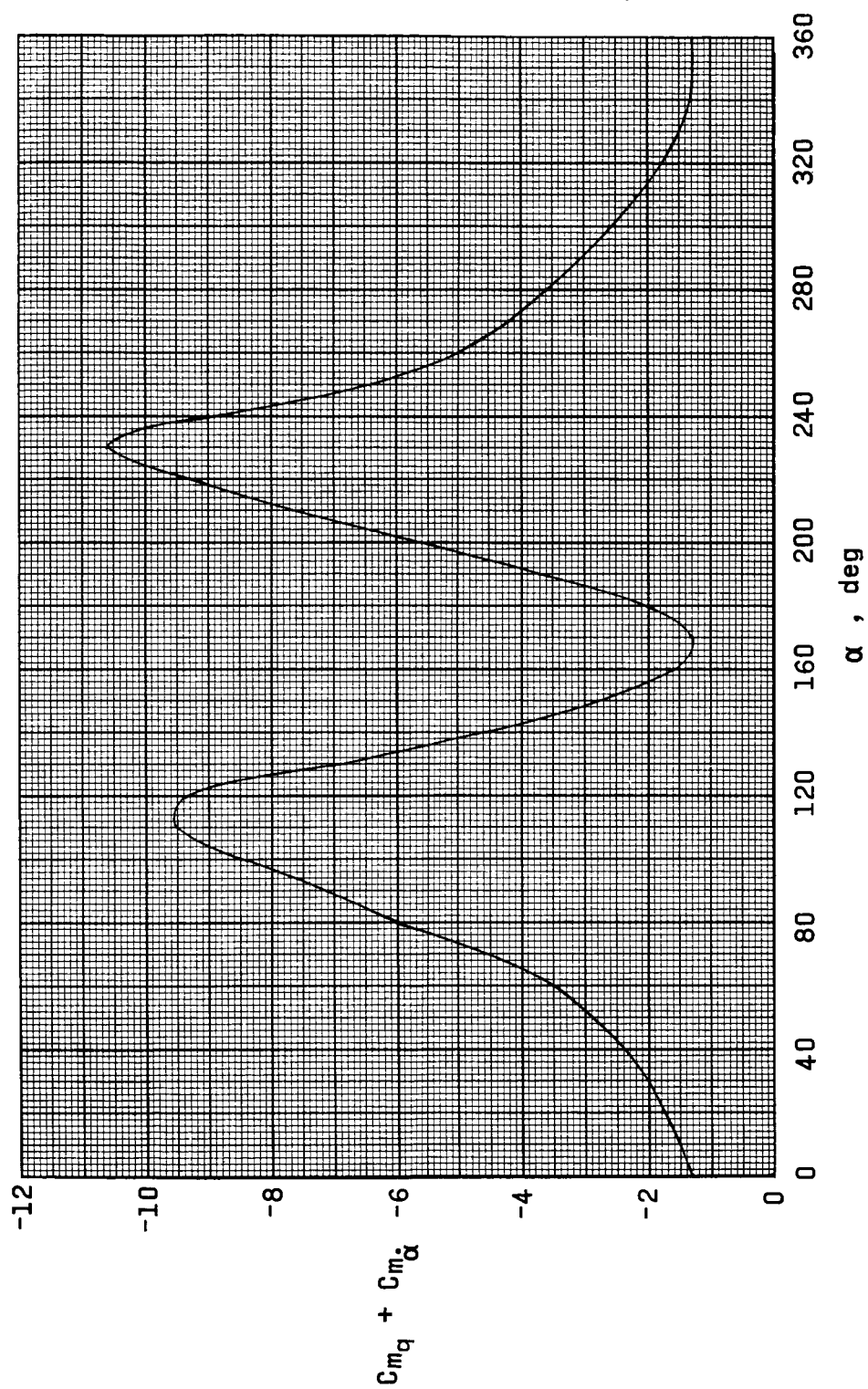
(d) Mach number = 1.5.

Figure 8.- Continued.

~~CONFIDENTIAL~~

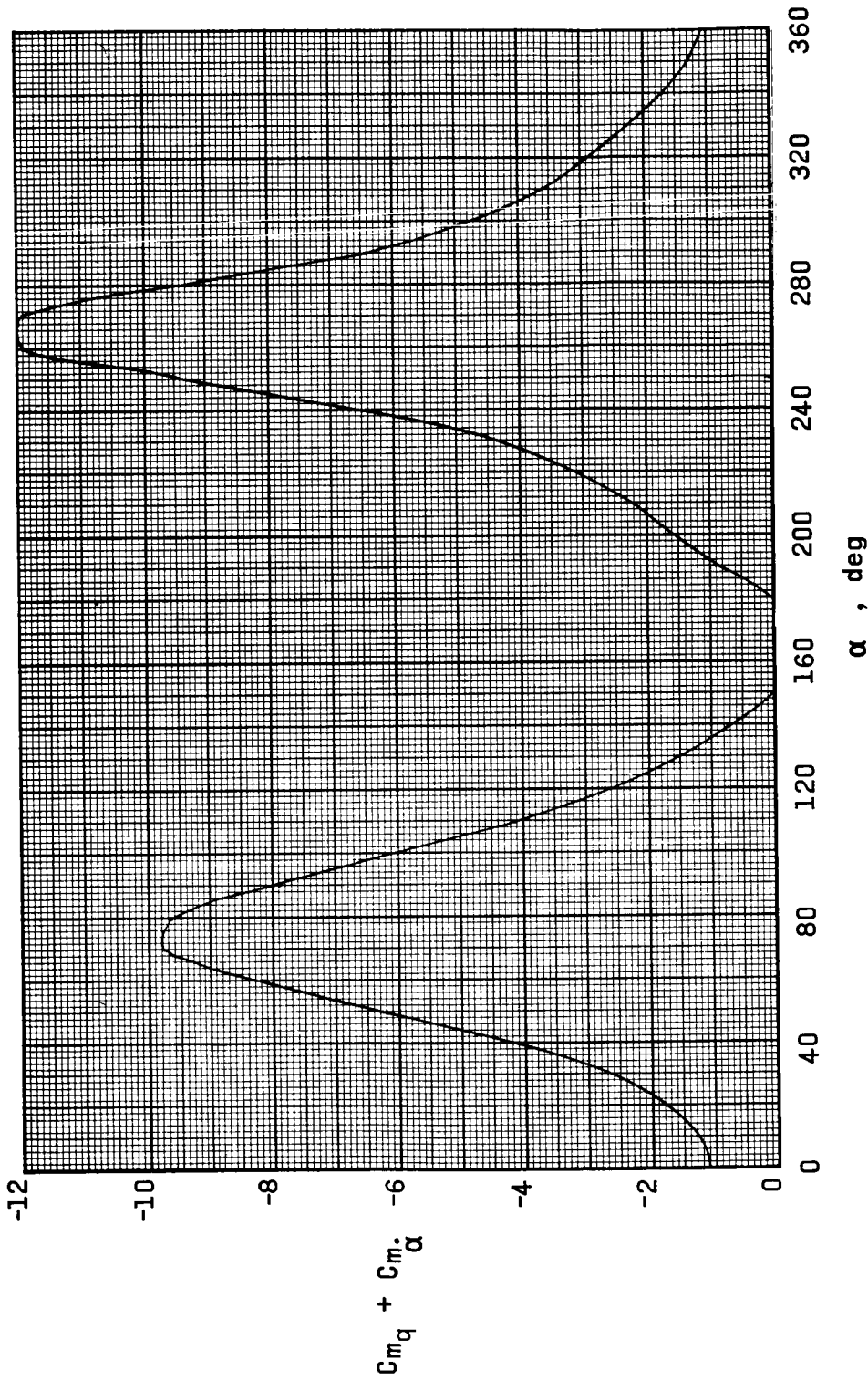
(e) Mach number = 2.0.

Figure 8.- Continued.



(f) Mach number = 3.0.

Figure 8.- Continued.



(g) Mach number = 4.5.

Figure 8.- Concluded.